Reprinted from the *Journal* of the Institution of Engineers (India) vol 54, CI 4 March 1974

UDC 626.81

Design of Channel Transitions in Supercritical Flows

R Jayaraman, *Non-member*
Dr V Sethuraman, *Member*

This paper deals with the design of supercritical transitions—both expansions and contractions. The design procedure based on the gas dynamics analogy is presented with the help of design charts prepared by the authors in a form suitable for direct use by the practising engineer. The limitations of the analogy are pointed out and the scope for further work in the field is indicated.

INTRODUCTION

Steep high-velocity channels are often employed in flood escapes, spillways, chutes, etc. Occasionally, steep lined channels are used in tunnels and in rocky terrain so as to reduce the cost of excavation. When a steep-sloped channel takes off from a sluice-gate it is often economical to have a restricted waterway for the sluices and allow the water to expand through a transition. Similarly, when a steep-sloped channel passes through an aqueduct or tunnel, inlet and outlet transitions become necessary. Supercritical transitions are also necessary when changes in the general ground slopes dictate changing a narrow, deep and steep channel to a wider, shallower and less steep channel or *vice versa*.

Transitions for subcritical flow are designed for minimum energy loss and a smooth water surface profile by proper streamlining of the sides and the bottom; transitions for supercritical flow for minimum wave-heights and least disturbances in the flow downstream of the transition. An improperly designed high-velocity transition will exhibit standing waves of excessive height and severe disturbances which not only pose the threat of overtopping of the channel but also lead to appreciable energy loss. The disturbances will persist for a long distance downstream by reflection from the side walls and increase the risk of erosion of the lining of the channel. Proper shaping of the transition is thus a matter of prime importance in the operation of steep channels.

Papers dealing with high velocity flow through transitions published in the past, are not in a form suitable for direct use by the practising engineer. In this paper, the design aspects of supercritical transitions—both expansions and contractions—are presented in a consolidated form with charts prepared by the authors and illustrated by numerical examples.

MECHANICS OF WAVE FORMATION

It was Preiswerk[1] who first applied the principles of gas dynamics relating to supersonic flow for the study of supercritical open channel flows. Blaisdell adopted his method in 1944 for the graphical construction of the flow in a transition. The analysis and design of supercritical transitions was put on a sound footing in 1949 when Ippen[2,3], Rouse[4], Knapp[5] and others contributed papers at a Symposium on High-Velocity Flow.

According to the gas dynamics analogy, a supercritical flow experiences the effect of a wall deflection only by means of 'disturbance lines' originating from the point or zone of wall deflection or curvature. Consider, for example, an abrupt outward deflection of the wall [Fig 1(i)]. A series of negative disturbance lines, or the Mach lines in gas dynamics, originate at the point of the wall deflection. As the streamlines cross the group of disturbance lines (sometimes referred to as the 'expansion fan'), the water level falls gradually while the Froude number increases correspondingly. The first disturbance line is inclined at the Mach angle $\beta_1 = \sin^{-1}\left(\frac{1}{F_1}\right)$ to the streamline, while the last disturbance line is inclined at the Mach angle $\beta_2 = \sin^{-1}\left(\frac{1}{F_2}\right)$ to the deflected flow. It may be noted here that the intermediate disturbance lines are imaginary lines and may be thought of as discretized water surface contours. In an actual problem, the total flow deflection may be divided into steps of, say, 2° and the corresponding disturbance lines located. In any zone bounded by discretized disturbance lines, the flow properties such as depth of flow and the Froude number are assumed to be constant. Except for a localized region near point O, the water surface slopes are not large. Hence, there is not wave formation as such and energy loss due to the flow expansion is negligible.

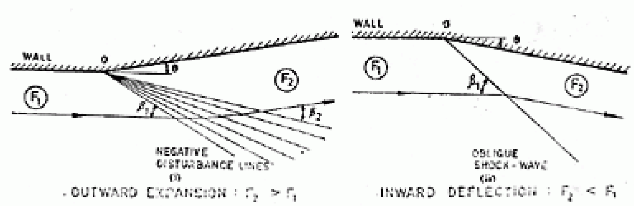

Fig 1

Consider the inward deflection of the wall by an angle θ [Fig 1(ii)]. As in supersonic gas flow, this gives rise to a shock wave, which manifests itself on the water surface as an oblique standing wave of appreciable height. The shock wave is obviously accompanied by

R Jayaraman and Dr V Sethuraman are with Hydraulic Engineering Laboratory, Indian Institute of Techonology, Madras.

This paper was received on December 19, 1972 and was presented and discussed at the Semi-Annual Paper Meeting held at Calcutta on December 3, 1973. Written discussion on this paper will be received until May 31, 1974.

some energy loss. The depth of flow is increased below the shock wave while the Froude number is reduced. These can be evaluated by applying the momentum principle to the oblique standing wave. However, an inward wall deflection of very small value (say, a few degrees), producing a 'weak shock', may be thought of as giving rise to a solitary positive disturbance line that may be analyzed by the same methods as for outward wall deflection.

A simple analysis of the 'weak wave' (both negative and positive) may be made on the following assumptions :

(1) The disturbances are small ;
(2) Vertical components of velocity are negligible ;
(3) Hydrostatic pressure distribution prevails over the depth of flow at every point ;
(4) Energy dissipation due to friction and wave-formation is negligible ; and
(5) Bottom shear is assumed to be balanced by the component of the gravity force.

Consider a small inward deflection $d\theta$ of a supercritical flow by means of a weak wave having an obliquity β_1 with respect to the initial flow direction [Fig 2(i)]. Let the velocities of flow before and after crossing the wave be V_1 and V_2. Resolving the velocities into components normal and tangential to the wave, $V_{t2} = V_{t1}$ since the wave can affect only the momentum normal to it. The continuity equation is

$$h_1 V_{n1} = h_2 V_{n2}$$

The momentum equation is

$$\tfrac{1}{2} w h_2^2 - \tfrac{1}{2} w h_1^2 = \frac{w q}{g} (V_{n1} - V_{n2})$$

$$V_{n1} = \sqrt{g h_1} \sqrt{\tfrac{1}{2} \frac{h_2}{h_1}\left(1 + \frac{h_2}{h_1}\right)} \qquad (1)$$

This expression is identical to the expression for the celerity of a gravity surge in a channel.

In the limiting case of a weak wave, $h_2 = h_1$ and $V_{n1} = \sqrt{g h_1}$. Hence,

$$\beta_1 = \sin^{-1} \frac{\sqrt{g h_1}}{V_1} = \sin^{-1} \frac{1}{F_1} \qquad (2)$$

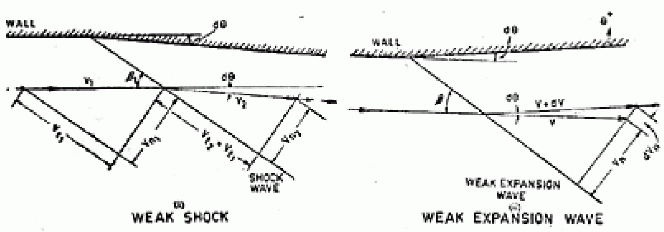

Fig 2

It follows that any continuous disturbance or weak wave in a supercritical flow orients itself to the flow such that the component of the flow velocity normal to the wave equals the critical velocity $\sqrt{g h_1}$. Here there is a striking analogy with supersonic gas flow in that any Mach line in a supersonic gas flow also orients itself to the flow such that the component of the flow velocity normal to the waves equals the speed of sound.

The change in depth of flow and Froude number caused by the deflection of the flow can now be computed. For a weak expansion wave [Fig 2(ii)],

$$dV_n = \frac{V\, d\theta}{\cos \beta}$$

The momentum equation is

$$\tfrac{1}{2} w h^2 + \frac{w}{g} q V_n = \text{Constant}$$

Differentiating,

$$dV_n = -\frac{g}{V_n} dh$$

Equating the two expressions for dV_n,

$$\frac{V\, d\theta}{\cos \beta} = -\frac{g\, dh}{V_n}$$

$$\frac{dh}{d\theta} = \frac{V V_n}{g \cos \beta} = -\frac{V^2}{g} \tan \beta$$

Since there is no energy loss, $V = \sqrt{2 g (H - h)}$.

Substituting for V and $\tan \beta$, we get

$$\frac{dh}{d\theta} = \frac{2 g (H - h)}{g} \frac{\sqrt{h}}{\sqrt{2 H - 3 h}} = -\frac{\sqrt{\frac{2h}{H}}\left(1 - \frac{h}{H}\right)}{\sqrt{1 - \frac{3}{2}\frac{h}{H}}} H$$

Integrating,

$$\theta = \left\{ \sqrt{3} \tan^{-1} \sqrt{\frac{1 - \frac{3}{2}\frac{h}{H}}{\frac{3}{2}\frac{h}{H}}} - \tan^{-1} \sqrt{\frac{3\left(1 - \frac{3}{2}\frac{h}{H}\right)}{\frac{3}{2}\frac{h}{H}}} \right\} - \theta_1$$

where the constant of integration θ_1 is the value of the term within parenthesis for $h = h_1$.

Introducing the Froude number, $\dfrac{h}{H} = \dfrac{2}{2 + F^2}$,

$$\theta = \sqrt{3} \tan^{-1} \sqrt{\frac{F^2 - 1}{3}} - \tan^{-1} \sqrt{F^2 - 1} - \theta_1 \quad (3)$$

It is convenient to introduce here the 'dimensionless velocity of flow' $\bar{V} = \dfrac{V}{\sqrt{2 g H}}$.

$$\bar{V}^2 = \frac{F^2}{2 + F^2}\ ;\ F^2 = \frac{2 \bar{V}^2}{1 - \bar{V}^2} \qquad (4)$$

$$\theta = \sqrt{3} \tan^{-1} \sqrt{\frac{3 \bar{V}^2 - 1}{3 (1 - \bar{V}^2)}} - \tan^{-1} \sqrt{\frac{3 \bar{V}^2 - 1}{1 - \bar{V}^2}} - \theta_1 \qquad (5)$$

If θ_1 is ignored and $\bar{V}$ is plotted against θ, using polar coordinates, the resulting curve is an epicycloid between the circles of radii $\dfrac{1}{\sqrt{3}} = 0.577$ and 1, and occupying a vectorial angle $\theta = 65°53'$.

When $F = 1, \bar{V} = 0.577, \theta = 0°$

When $F = \infty, \bar{V} = 1, \theta = 65°53'$

If the complete family of the left-running and right-running epicycloids are drawn for θ varying by a small increment of about 2°, we get the 'characteristics diagram' (Fig 3). At every point in the flow, the characteristics of the left-running and right-running families of curves are inclined at an angle of $\sin^{-1}\frac{1}{F}$ to the flow direction. In physical terms, the characteristics define the directions of propagation of an elementary disturbance on the surface at the point under consideration.

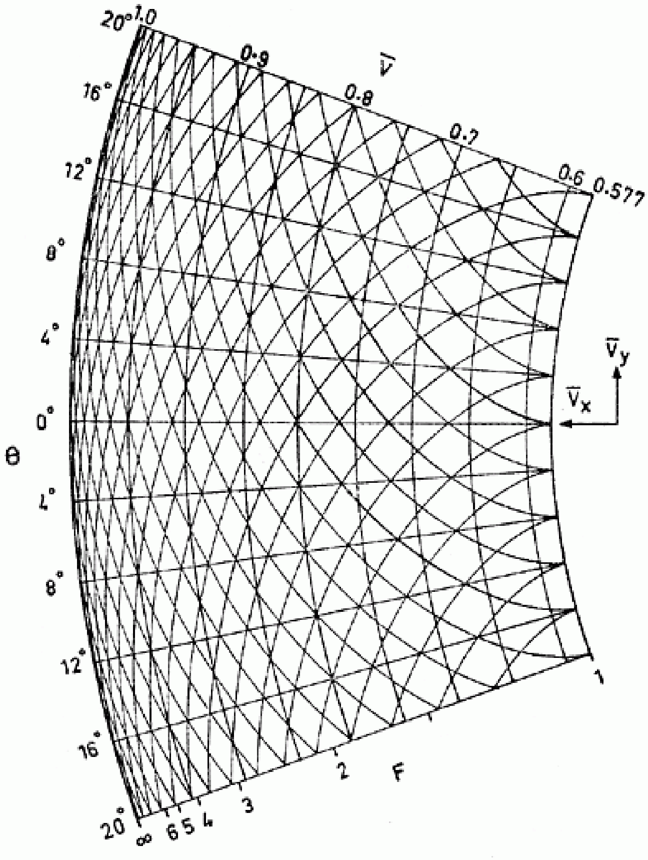

Fig 3 Characteristics diagram

In solving a problem, the initial point in the diagram is chosen on the $\bar{V}_x$ axis (θ = 0°) with the appropriate value of $\bar{V}$. If the boundary deflects through an angle of θ, then starting from the initial point, one of the epicycloidal branches leading inward or outward is followed, according as whether the disturbance is positive or negative, till it intersects the radial line corresponding to θ. The radius vector to this point gives the new value of $\bar{V}$.

The direction of the corresponding disturbance line can be shown to be that of the normal at the mid-point of the epicycloidal arc just traversed. This can be easily located by using an elliptical template, known as the Mach ellipse, having its semi-axes equal to $\bar{V}=1$ and $\bar{V}=0.577$, respectively. If the Mach ellipse is centred on the characteristics diagram in such a way that the point on the characteristics diagram falls on it, the major axis of the ellipse will represent the direction of the disturbance lines.

The application of the 'method of weak waves' for the construction of the flow in a transition requires the establishment of rules governing wave interaction, like those in gas dynamics. These rules are :

(1) A positive or negative wave gets reflected from a straight wall as a positive or negative wave of the same strength [Fig 4(i)]. Here the strength of a wave is reckoned by the flow deflection which it is capable of producing. The direction of the reflected wave can be obtained from the characteristics diagram. It may be noted that the incident and reflected waves are not equally inclined to the straight wall.

(2) If the waves intersect, they cross over and proceed with undiminished strength. But the wave fronts suffer refraction as shown in Fig 4(ii). The orientations of the waves can be worked out from the characteristics diagram.

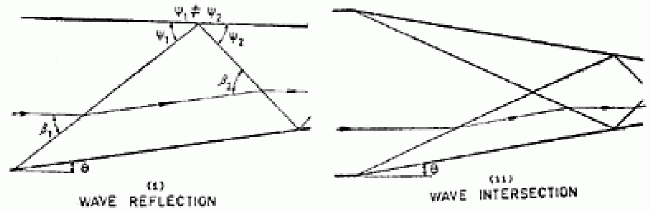

Fig 4

While the gas dynamics analogy is no doubt interesting, its limitations should not be lost sight of. In a supersonic flow, every particle of the flow is moving at a velocity exceeding that of a pressure wave and hence may be thought of as a potential source for a Mach wave or a shock wave. On the other hand, in supercritical flow of water, the velocity of flow exceeds only the celerity of a solitary gravity wave of low height on the surface of the flow. The velocity of flow is evidently nowhere near the velocity of sound in water ; Unlike the case of supersonic flow of a gas, the special effects in a supercritical flow of water are only surface effects. For example, a pitot tube immersed in a water flow will have almost the same coefficient in subcritical and supercritical flows, whereas a pitot tube inserted in a gas flow will have quite different coefficients for subsonic and supersonic flow regimes. Other factors which limit the usefulness of the gas dynamics analogy are : fluid viscosity and the associated boundary layer effects on the gravity waves, and surface tension, giving rise to capillary waves. The finite height of the waves and the small depth of flow further complicate the phenomenon. Nevertheless, the gas dynamics analogy gives quite useful results when applied to the design of supercritical transitions.

APPLICATION OF THE METHOD OF WEAK WAVES TO THE DESIGN OF EXPANSIONS

It is possible to design a supercritical expansion in such a way that: (1) there is no separation of the high-velocity sheet in the transition ; (2) shock waves are absent; and (3) the negative disturbances created by the initial outward wall deflection are cancelled as they reach the opposite wall, so that the flow beyond the transition will be free from disturbances. The ideal expansion thus consists of: (1) on initial expansion AB (Fig 7) of a reasonably good shape that lies within the boundary profile of a freely expanding rectangular jet at the same Froude number; (2) a straight tangent at the peak wall inclination θ_{max} up to C where the first wave from the opposite wall meets the tangent BC ; and (3) a 'region of wave cancellation' CD in which the negative waves from the opposite wall are just cancelled by an appropriate inward wall deflection. Because of the symmetry, the centre line of the channel can be thought of as an imaginary wall giving rise to wave reflection, as shown in Fig 7.

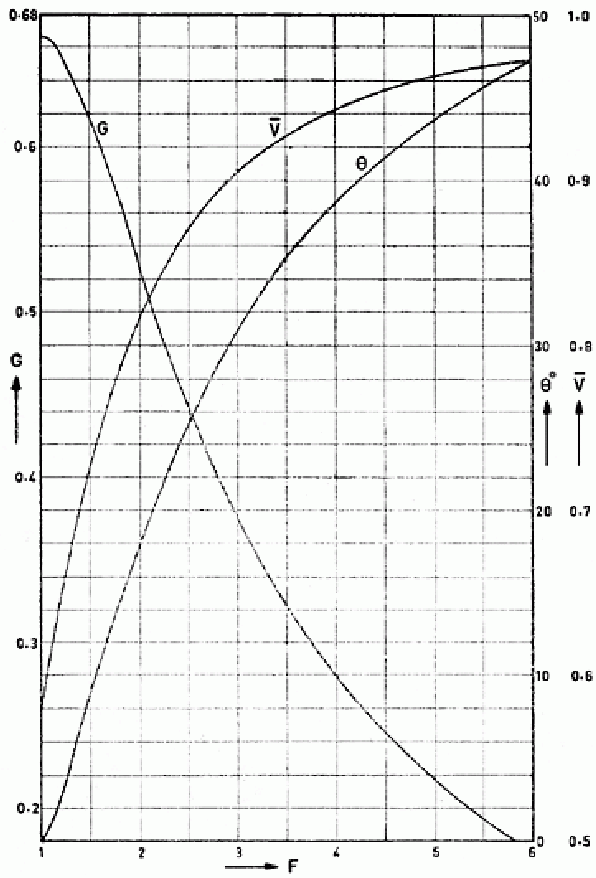

Fig 5 Design chart for supercritical expansions

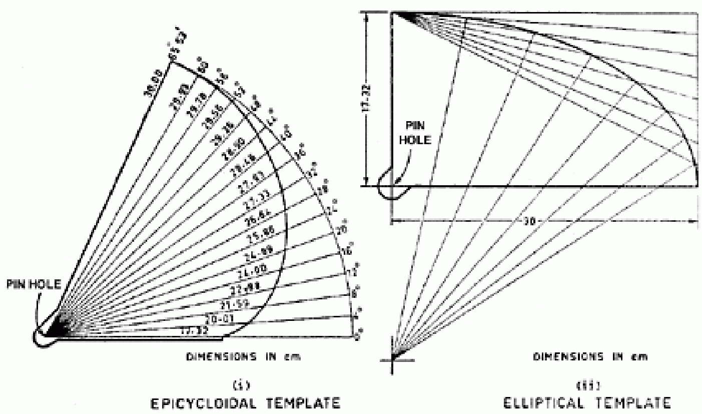

Fig 6

Based on his experiments on the free expansion of rectangular supercritical jets, Rouse[4] suggested that the initial expansion profile may be taken as

$$\frac{y}{b_1} = k\left(\frac{x}{b_1 F_1}\right)^{\frac{3}{2}} + \frac{1}{2} \qquad (6)$$

The constant k can be varied from $\frac{1}{2}$ to $\frac{1}{8}$ according as whether a short or a long (and better) transition is desired.

Although the method of weak waves is based on the questionable assumptions of zero friction and zero bed slope, these two effects are to some extent mutually cancelling, with the result that the results given by this method are sufficiently accurate for most practical purposes. Given the initial flow conditions and the final width at the end of the expansion, the conventional method of design involves the choice of a trial value of the peak wall deflection θ_{max}, the determination of the corresponding final width on the basis of wave cancellation, and trial and error adjustment of θ_{max} such that the computed final width equals the given final width. A more straightforward design procedure, not involving any trial and error, has been given. A new function G has been introduced so that F_2 can be computed directly.

Applying the continuity equation to the flow upstream and downstream of the transition,

$$b_1 h_1^{\frac{3}{2}} F_1 = b_2 h_2^{\frac{3}{2}} F_2$$

$$\frac{h_2}{h_1} = \left(\frac{b_1 F_1}{b_2 F_2}\right)^{\frac{2}{3}}$$

Since energy losses are neglected,

$$h_1 \left(1 + \tfrac{1}{2} F_1^2\right) = h^2 \left(1 + \tfrac{1}{2} F_2^2\right)$$

$$\frac{h_2}{h_1} = \frac{1 + \frac{1}{2} F_1^2}{1 + \frac{1}{2} F_2^2}$$

Equating the two expressions for $\frac{h_2}{h_1}$ and rearranging the terms,

$$\frac{F_2}{1 + \frac{1}{2} F_2^2} = \frac{F_1^{\frac{2}{3}}}{1 + \frac{1}{2} F_1^2} \frac{1}{\left(\frac{b_2}{b_1}\right)^{\frac{2}{3}}}$$

Denoting the function $\frac{F^{\frac{2}{3}}}{1 + \frac{1}{2} F^2}$ as G,

$$G_2 = \frac{G_1}{\left(\frac{b_2}{b_1}\right)^{\frac{2}{3}}}$$

Making use of a graph of G *vs* F (Fig 5), G_2 can be computed, and hence the downstream Froude number F_2 is determined.

Equation (3) shows that any value of the Froude number is associated with a corresponding value of the function $\theta(F)$. Hence, the Froude number increases from F_1 to F_2 calls for a total flow deflection of $(\theta_2 - \theta_1)$, where $\theta_2 = \theta(F_2)$ and $\theta_1 = \theta(F_1)$. But the final flow is obviously in the same direction as the initial flow. It follows that half of $(\theta_2 - \theta_1)$ is brought about by the negative waves originating from the initial expansion, while the remaining half is accounted for as the flow crosses the reflected negative waves and is brought back to the axial direction. Hence, the peak flow deflection, given by $\theta_{max} = \frac{1}{2}(\theta_2 - \theta_1)$, is also determined.

The graph of θ *vs* F (Fig 5) helps the evaluation of θ_{max}.

The remainder of the design consists in fixing the complete wall profile ABCD and constructing the wave pattern of the flow in the expansion.

BLAISDELL'S GRAPHICAL METHOD FOR THE CONSTRUCTION OF THE FLOW IN EXPANSIONS

In 1944, Blaisdell[6] presented a graphical procedure for the construction of supercritical flow in transitions by the method of characteristics. Two templates are needed (Fig 6) for applying this method, and may be cut out of 3 mm perspex sheet. The figure also gives the polar coordinates of the epicycloidal curve for a maximum radius vector of 30 cm.

It is best to describe the graphical procedure with respect to the specific example of a curved supercritical

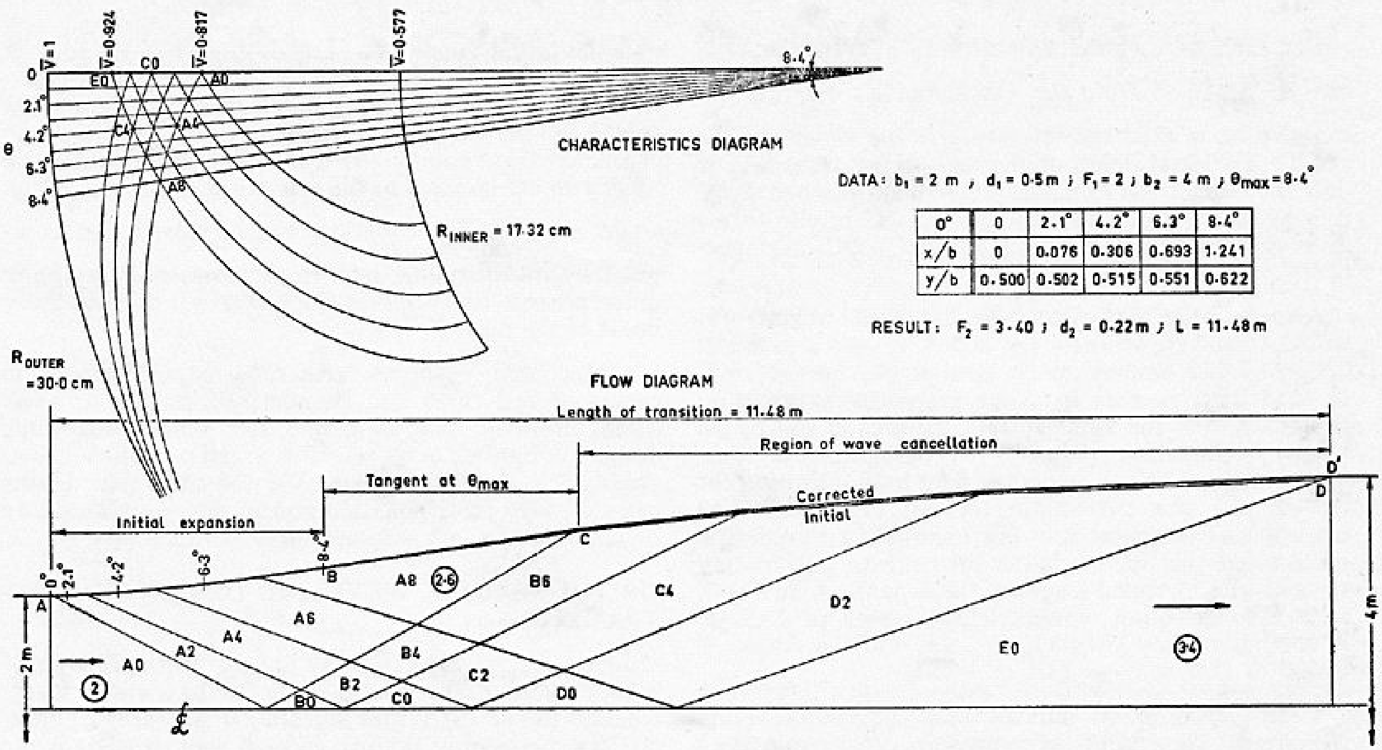

Fig 7 Design of a supercritical expansion

expansion. The zone numbering system described here is somewhat more meaningful than that originally proposed by Blaisdell. All the weak waves considered in a problem are of equal strength, capable of a flow deflection of approximately 2°. The exact value will depend on the value of θ_{max}. In Fig 7, A0 represents the initial flow. As the initial expansion of the boundary turns the flow, the flow passes through zones A_2, A_4, etc, the number always representing the approximate inclination of the flow to the axial (or initial) direction. When the flow crosses the reflected waves, the prefix A changes to B, C, etc. For example, in zone D_2, the flow has crossed three reflected waves and is inclined at nearly 2° to the axis.

EXAMPLE

Design a supercritical expansion, given $b_1 = 2$ m, $d_1 = 0.5$ m, $b_2 = 4$ m, and $F_1 = 2$.

$F_1 = 2.0$. Referring to Fig 5, $G_1 = 0.528$ and $G_2 = 0.528 \times 0.5^{0.67} = 0.333$.

Referring to the graph, $F_2 = 3.40$.

Again, from Fig 5, $\theta_1 = 18.0°$ and $\theta_2 = 34.6°$. Therefore, $\theta_{max} = \frac{34.6 - 18.0}{2} = 8.3°$.

This is rounded off to 8.4° so that the total wall deflection may be considered in 4 steps of 2.1° each. This exact value of $\theta = 8.4°$ will be used in the graphical construction, but it will be taken as 8° for purposes of zone numbering.

The initial expansion follows the expression in equation (6). Assuming $k = \frac{1}{4}$,

$$\frac{y}{b_1} = \frac{1}{4}\left(\frac{x}{b_1 F_1}\right)^{\frac{3}{2}} + \frac{1}{2}$$

Differentiating,

$$\frac{dy}{dx} = \tan\theta = \frac{3}{8F_1}\left(\frac{x}{b_1 F_1}\right)^{\frac{1}{2}}$$

The initial expansion is divided into 4 arcs of 2.1° each. By putting $\theta = 2.1°$, 4.2°, etc in the above expression, x and y can be solved.

In Fig 7, A0 represents the initial flow. As the flow expands, we move to A8 on the diagram. Thereafter as the flow crosses the reflected waves, we move back to E0 on the characteristics diagram. A0-A8-E0 is the zone of interest in the characteristics diagram and is filled up with the left- and right-running characteristics at intervals of 2.1°.

As the boundary deflects through an angle of 2.1°, the flow properties correspond to A2 on the characteristics diagram. The corresponding disturbance line is drawn on the flow diagram, starting from the point of mid-slope of the wall, and parallel to a normal to the arc A0-A2 of the characteristics diagram at the mid-point of the arc. When this disturbance line reaches the imaginary wall at the axis of the channel, it gets reflected as a new negative wave. The graphical construction progresses step-by-step, as the primary and reflected waves interact in the flow diagram producing wave refraction. When the first reflected wave reaches the wall at point C on the tangent BC inclined at θ_{max}, the region of wave cancellation begins. At C, the boundary is turned inwards by 2.1° so that the negative wave which would otherwise have been produced by reflection of the incident wave is just cancelled out by the positive wave which would normally result from an inward wall deflection. Finally, the wall is brought back to the axial direction at D.

Check whether the final width at the end of the expansion is equal to b_2. If there is any slight discrepancy, the necessary correction to the expansion profile can be easily made graphically. Starting from the end of the expansion, D is shifted to D′ (Fig 7) and the corrected segments of the wall profile are drawn backwards, such that they are parallel to the corresponding original segments. When the profile reaches the initial expansion zone, the readjustment necessary will be barely discernible.

For each zone of the flow diagram, $\bar{V}$, and hence F can be obtained from the characteristics diagram. $\frac{h}{h_1}$ can also be worked out so as to give the water surface profile. The final depth at the end of the transition is only 0.44 times the initial depth. Unless the bed slope is increased beyond the transition, a S3 profile forms after the transition, attaining normal depth asymptotically.

Although the above example has been worked out with 2.1° wall elements for the sake of clarity, a practical design should employ much smaller elements of 0.5° or so. It may be seen from the graphical construction that the smaller the wall elements, the greater will be the length of transition indicated by the graphical construction. In order to correct the length of transition for the element size, the limiting or last disturbance line originating from point B in Fig 7 should be traced. The point where this line meets the downstream wall beyond D yields the corrected length of the expansion. In Fig 7, such a construction would yield a length of 13.2 m. A computer study gives θ_{max} as 8.23° and the corrected length of expansion as 13.1 m.

Recent experiments indicate that the low-curvature region near the end of the expansion can be shortened by as much as 10% of the corrected length of expansion without significantly affecting the performance of the expansion. The factors that critically affect the performance of the expansion are θ_{max}, the correct location of point C and the correct shaping of the wave-cancellation region immediately following, and in the vicinity of C.

RIGOROUS SOLUTION FOR THE SUPERCRITICAL FLOW IN EXPANSIONS

Given the boundary geometry of an expansion, supercritical flow in the expansion can be analyzed rigorously taking into account the bed slope of the transition and frictional loss. However, the analysis cannot normally be applied to contractions because of the formation of shock waves in contractions.

Assuming two-dimensional planar flow with negligible vertical acceleration and hydrostatic distribution of pressure, the differential equations become[7]

$$u \frac{\partial h}{\partial x} + h \frac{\partial u}{\partial x} + v \frac{\partial h}{\partial y} + h \frac{\partial v}{\partial y} = 0 \qquad (7)$$

$$u \frac{\partial u}{\partial x} + v \frac{\partial u}{\partial y} + g \frac{\partial h}{\partial x} = g\,(S_0 - S_{fx}) \qquad (8)$$

$$u \frac{\partial v}{\partial x} + v \frac{\partial v}{\partial y} + g \frac{\partial h}{\partial y} = - g\, S_{fy} \qquad (9)$$

where x and u are the coordinate and the velocity in the downstream direction, y and v the coordinate and the velocity in the lateral direction, h is the depth of flow, g the acceleration due to gravity, S_0 the channel slope, and S_{fx} and S_{fy} are the component friction slopes in x and y directions. Adopting Chezy's formula for the friction slope,

$$S_{fx} = \frac{u\sqrt{u^2 + v^2}}{C^2\, h} \qquad (10)$$

$$S_{fy} = \frac{v\sqrt{u^2 + v^2}}{C^2\, h} \qquad (11)$$

The dependent variables are u, v, h, which are unique functions of x and y, defined by the boundary geometry and the initial conditions. Equations (7) to (9) form a set of quasi-linear hyperbolic partial differential equations, and reduce to a three-characteristic problem when solved by the method of characteristics. Of the three characteristics, one is the streamline itself while the other two are inclined to the velocity vector at the Mach angle $\sin^{-1} \frac{1}{F}$. The equations can be solved in a computer by transforming them to the corresponding finite difference equations. The solution gives u, v and h at every point of the flow.

Liggett and Vasudev[8] have reported that since the effects of bed slope and channel friction are to some extent mutually cancelling, the 'frictionless, zero-slope design' is entirely adequate for practical problems on gradual channel expansions. The velocities and depths calculated by the simple method of characteristics may be relied upon to an accuracy of 10% or so.

OBLIQUE SHOCK WAVE AND DESIGN OF CONTRACTIONS

Just as in gas dynamics, an inward wall deflection of a high velocity flow usually gives rise to a shock wave, whether the flow is turned suddenly or somewhat gradually. In the case of gradual inward wall deflection, the positive disturbance lines converge downstream and eventually merge into a shock-wave. The shock-wave manifests itself as an oblique hydraulic jump accompained by energy loss.

We have seen that the obliquity of a standing wave can be written as

$$\sin \beta_1 = \frac{1}{F_1} \sqrt{\tfrac{1}{2} \frac{h_2}{h_1} \left(1 + \frac{h_2}{h_1} \right)} \qquad (12)$$

Solving for $\frac{h_2}{h_1}$, we get

$$\frac{h_2}{h_1} = \tfrac{1}{2}\, [\sqrt{1 + 8\, F_1^2 \sin^2 \beta_1} - 1] \qquad (13)$$

Also, $V_{n1} = V_{t1} \tan \beta_1$; $V_{n2} = V_{t2} \tan (\beta_1 - \theta)$; $V_{t1} = V_{t2}$; and $h_1 V_{n1} = h_2 V_{n2}$. So,

$$\frac{h_2}{h_1} = \frac{\tan \beta_1}{\tan (\beta_1 - \theta)} \qquad (14)$$

Combining equations (13) and (14),

$$\frac{h_2}{h_1} = \tfrac{1}{2}\, [\sqrt{1 + 8 F_1^2 \sin^2 \beta_1} - 1] = \frac{\tan \beta_1 + \tan \theta \tan^2 \beta_1}{\tan \beta_1 - \tan \theta} \qquad (15)$$

$$\tan \theta = \frac{\tan \beta_1 \left[\sqrt{1 + 8\, F_1^2 \sin^2 \beta_1} - 3 \right]}{2 \tan^2 \beta_1 - 1 + \sqrt{1 + 8\, F_1^2 \sin^2 \beta_1}} \qquad (16)$$

$$F_2 = \sqrt{\frac{h_1}{h_2} \left[F_1^2 - \tfrac{1}{2} \frac{h_1}{h_2} \left(\frac{h_2}{h_1} - 1 \right) \left(\frac{h_2}{h_1} + 1 \right)^2 \right]} \qquad (17)$$

It may be noted that when $\beta_1 = 90°$, the equations for the normal hydraulic jump are obtained.

$$\frac{h_2}{h_1} = \tfrac{1}{2}\, [\sqrt{1 + 8\, F_1^2} - 1]$$

$$F_2 = \frac{F_1}{[\tfrac{1}{2}\, (\sqrt{1 + 8\, F_1^2} - 1)]^{\frac{3}{2}}}$$

It is interesting to plot the variation in the value of the dimensionless velocity $\overline{V}$ through an oblique jump (Fig 8). Let A represent the initial value of the dimensionless velocity $\overline{V}_1$. If a wall deflection θ produces an oblique jump, point B will represent $\overline{V}_2$ after the jump. The locus of point B for various values of θ gives rise to the curve shown in Fig 8, well-known as the 'shock polar' in gas dynamics. A circle with radius $\overline{V} = 0.577$ separates supercritical and subcritical flow regimes. Point C represents the flow condition below a normal hydraulic jump.

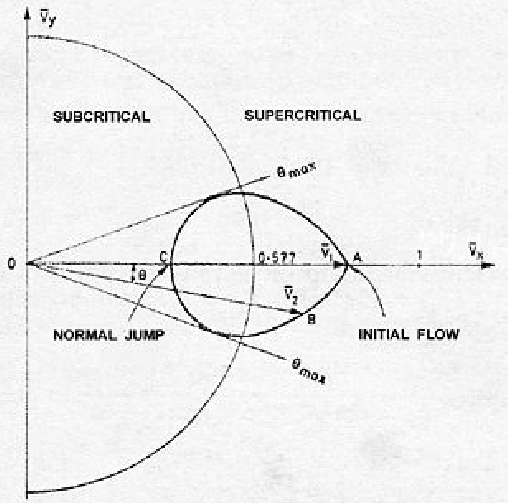

Fig 8 Shock-polar

The energy loss in the jump is given by $\triangle H = \dfrac{(h_2 - h_1)^3}{4\ h_1\ h_2}$.

For $\dfrac{h_2}{h_1} = 2$, $\triangle H$ is approximately $\frac{1}{8}\ h_1$. The result of the energy loss is that, if two successive flow deflections occur, the flow characteristics at the second deflection cannot be related to the initial shock polar.

Shock wave reflections and intersections occur in a manner more or less similar to that of weak waves.

Although the oblique shock wave is an interesting hydraulic phenomenon, it has not been studied in as much detail as its counterpart in gas dynamics. The actual obliquity of the shock wave in water has been found to be slightly different from the theoretical value, indicating the presence of secondary effects that have not been investigated in detail.

SHOCK-WAVE CHART

It is possible to prepare a set of charts giving the values of β_1, F_2 and $\dfrac{h_2}{h_1}$ for any given set of values of F_1 and θ. Such a chart (Fig 9) is quite helpful in the quick design of supercritical contractions.

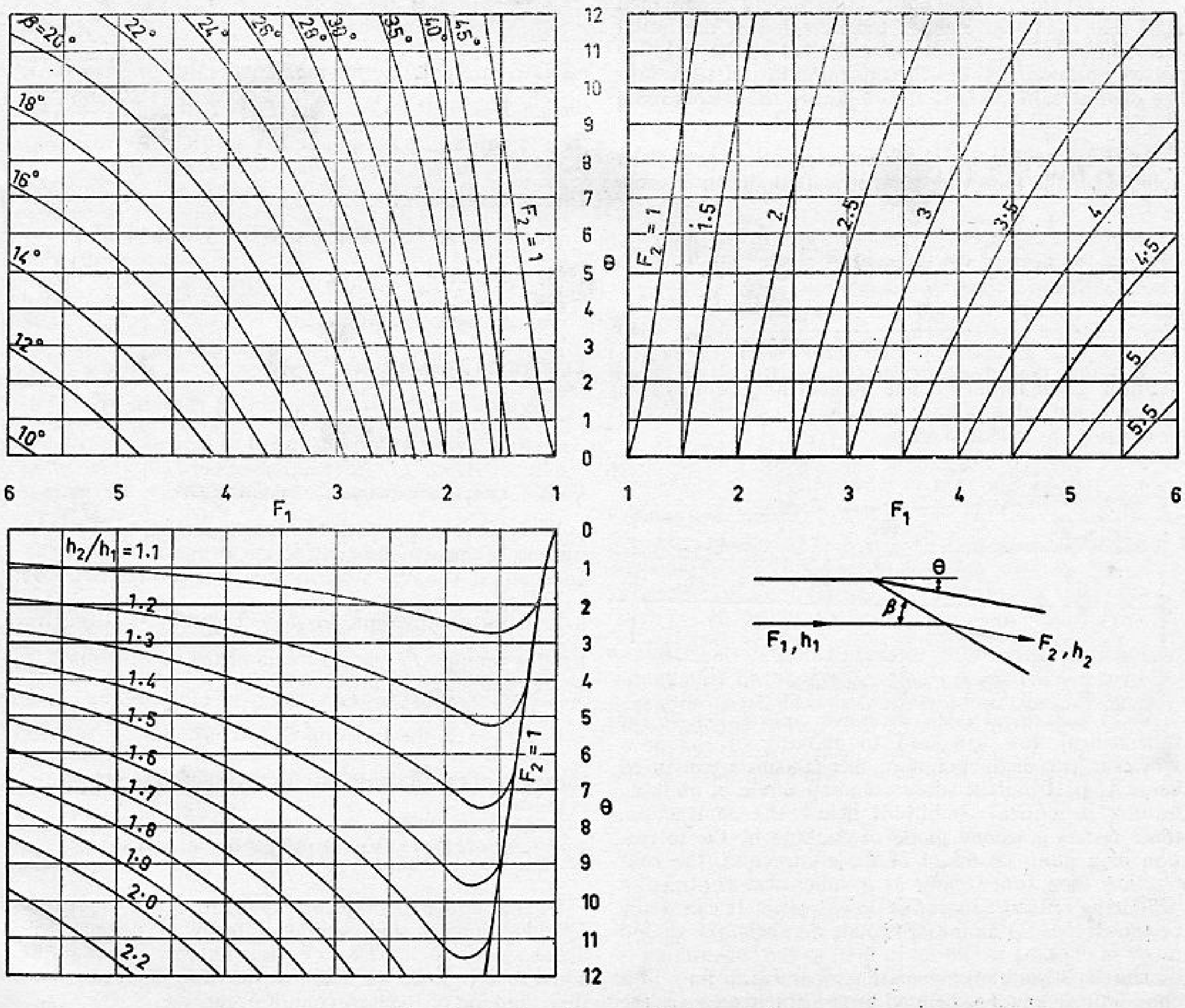

Fig 9 Design chart for supercritical contractions

DESIGN PROCEDURE FOR CONTRACTIONS

A practical supercritical contraction is invariably accompanied by a shock-wave, as it is not possible to eliminate the shock unless the contraction is made excessively long. Since the height of the shock wave is a function of the flow deflection, the prime design criterion is low peak deflection of the flow.

Typical side wall profiles for contractions are as shown in Fig 10. Since the straight contraction produces the least flow deflection in a transition of given length, straight contractions with a slight rounding off of the corners are preferable to curved contractions.

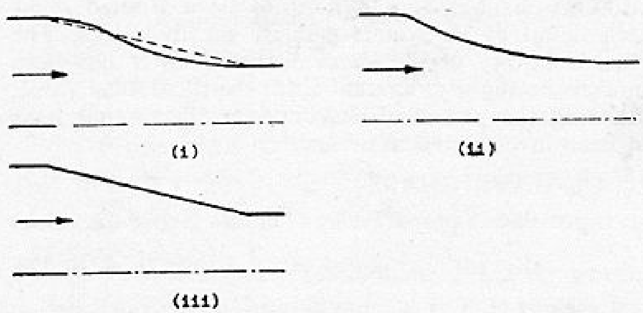

Fig 10 Contraction profiles

The ideal supercritical contraction should be designed such that the positive shock wave created by the initial inward turn of the wall is just cancelled by the negative waves produced by the subsequent outward turn into the downstream channel. Theoretically the downstream channel should then be free from waves.

Referring to Fig 11, shock-wave cancellation will be achieved if the following geometrical condition is satisfied.

$$\frac{b_1}{2}\cot\beta_1 + \frac{b_3}{2}\cot(\beta_2 - \theta) = \frac{b_1 - b_3}{2}\cot\theta$$

$$\frac{b_3}{b_1} = \frac{\cot\theta - \cot\beta_1}{\cot\theta + \cot(\beta_2 - \theta)} \qquad (18)$$

For a given initial Froude number and depth ratio, the optimum value of θ for shock-wave cancellation can be obtained by trial and error.

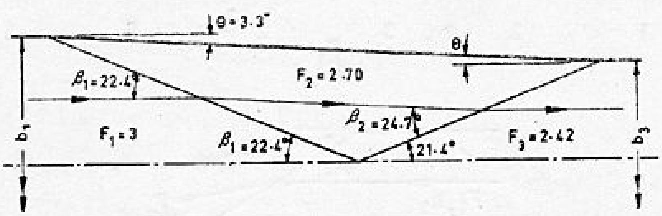

Fig 11 Contraction design

As in subcritical flow, excessive contraction of the supercritical flow can lead to choking of the flow. However, two distinct choking mechanisms are involved here. Apart from the more common mode of choking leading to critical conditions below the contraction, there occurs a second mode of choking by the formation of a jump upstream of the contraction, the contraction then functioning as a subcritical contraction producing critical conditions downstream. It can easily be shown that for all initial Froude numbers, the second mode of choking would set in first, as the constriction is increased. Since choking of the supercritical flow in a contraction may produce violent disturbances in the flow with the consequent risk of overtopping of the channel, it is desirable to make sure in the design that choking of the flow would not occur.

EXAMPLE

Design a straight supercritical contraction for $b_1 = 4$ m; $h_1 = 0.5$ m; $F_1 = 3$; and $b_3 = 3$ m.

The contraction ratio $\frac{b_3}{b_1} = 0.75$. The wall inclination should be evaluated by trial and error such that the computed value of $\frac{b_3}{b_1}$ also equals 0.75.

First Trial

Let $\theta = 3°$. Referring to the graphs in Fig 9 for $F_1 = 3$ and $\theta = 3°$, $\beta_1 = 22.2°$ and $F_2 = 2.72$ (by estimation). Again, for $F_2 = 2.72$ and $\theta = 3°$, $\beta_2 = 24.4°$ (by estimation).

$$\text{Computed } \frac{b_3}{b_1} = \frac{\cot 3° - \cot 22.2°}{\cot 3° + \cot (24.4 - 3)°} = 0.768$$

Second Trial

Let $\theta = 4°$. Proceeding as before, $\beta_1 = 23.2°$, $F_2 = 2.64$ and $\beta_2 = 25.8°$.

$$\text{Computed } \frac{b_3}{b_1} = 0.712$$

Now, interpolating for the actual value of $\frac{b_3}{b_1} = 0.75$, we get $\theta = 3.32° = 3.3°$, say. $F_2 = 2.70$ and $F_3 = 2.42$, $\frac{h_2}{h_1} = 1.19$, $\frac{h_3}{h_2} = 1.18$, and $\frac{h_3}{h_1} = 1.40$.

Check Continuity

$$b_1\, h_1^{1.5}\, F_1 = 4 \times 0.5^{1.5} \times 3 = 4.24$$

$$b_3\, h_3^{1.5}\, F_3 = 3\,(0.5 \times 1.40)^{1.5}\, 2.42 = 4.25$$

The expressions check well.

Length of Transition

The total length of the contraction is given by

$$L = \tfrac{1}{2}(b_1 - b_3)\cot\theta = 8.67 \text{ m}$$

Check for the Possibility of Choking

When the second mode of choking sets in, the Froude number F_3 below the contraction drops to 1, and the contraction behaves subcritically. Neglecting frictional loss in the contraction, for $F_3 = 1$ and $\frac{b_3}{b_1} = 0.75$, the Froude number F_2 just upstream of the contraction can be determined as follows:

For $F_3 = 1$, the function $G = 0.667$. For $\frac{b_3}{b_1} = 0.75$, the value of the function just upstream of the contraction is given by

$$G_2 = G_3\left(\frac{b_3}{b_1}\right)^{\frac{2}{3}} = 0.667 \times 0.826 = 0.551$$

By trial and error, the corresponding $F_2 = 0.48$. If this Froude number should prevail below a normal hydraulic jump, the upstream Froude number F_1 should be equal to 2.4. Since the actual value of F_1 is greater than this, choking of the flow cannot occur.

SCOPE FOR FURTHER WORK

Several aspects of supercritical flow in transitions need further experimentation to yield more refined guidelines for design.

The change in the Froude number associated with a supercritical transition is unfortunately just the opposite of what would generally be required. For example, the Froude number increases after an expansion designed as above, whereas an expansion is generally provided where it is desirable to increase the cross-section and reduce the bed slope and Froude number. Inevitably, supercritical transitions designed solely on the basis of wave interaction will give rise to S2 or S3 surface profiles in the downstream channel. It remains to be checked whether a suitable bed transition can be incorporated with the wall transition (as is normally done in subcritical transition) so as to eliminate the downstream surface profiles.

Another important aspect of the design of supercritical transitions is the 'Froude number sensitivity' of the design. Although uniform flow in a steep channel shows only a limited variation of the Froude number for a reasonably wide range of depths, yet some variation in the Froude number may have to be taken care of in the design. The conventional methods of design have the drawback that they achieve wave cancellaton and quiet flow only at the design Froude number. At other Froude numbers, the flow will exhibit standing waves and disturbances in the downstream channel.

Tursuno[9] has pointed out this drawback of a supercritical transition involving only a wall transition. He suggests the use of a curved bed transition in conjunction with the wall transition so as to make the design less dependent on the Froude number of the flow. It is proposed to experiment on this type of transition with a view to arrive at the design showing the least Froude number dependence.

The third aspect of the supercritical flow in a transition requiring advanced study is the effect of the channel roughness on the wave formation. It is well known that surface profiles in a transition computed by the elementary method of characteristics do not agree well with the actual profiles[10]. It is necessary therefore to make a critical comparison of the experimental surface profiles with the theoretical profiles obtained from a computer solution taking into account bed slope and channel friction.

Lastly, with regard to shock waves themselves, the actual inclinations of shock-waves in water are found to differ from the theoretical wave inclinations based on the shallow-water gravity wave theory. It may be that the discrepancy is the result of the action of the boundary layer and fluid viscosity, the effect of vertical accelerations or air-entrainment of the flow in the wake of the shock wave.

Experiments are now under way in the hydraulic engineering laboratory of the Indian Institute of Technology, Madras, on many aspects of the design of channel transitions for supercritical flow, with a view to suggesting better guidelines for design.

CONCLUSION

The design procedure for supercritical expansions and the graphical construction of the resulting wave pattern have been presented in an improved form which obviates the need for a trial and error solutton. New Design charts have been presented for the design of supercritical contractions. The limitations of the gas dynamics analogy in the design of supercritical transitions have been stressed, and the need for further experimentation pointed out.

REFERENCES

1. E Preiswerk. 'Application of the Methods of Gas Dynamics to Water Flows with Free Surface, Parts I and II'. NACA Technical Memorandum 934 and 935, 1940.

2. A T Ippen. 'Mechanics of Supercritical Flow—Symposium on High-Velocity Flow'. *Transactions of American Society of Civil Engineers*, 1951.

3. A T Ippen and J H Dawson. 'Design of Channel Contractions : Symposium on High Velocity Flow'. *Transactions of American Society of Civil Engineers*, 1951.

4. H Rouse, *et al.* 'Design of Channel Expansions Symposium on High Velocity Flow'. *Transactions of American Society of Civil Engineers*, 1951.

5. R T Knapp. 'Design of Channel Curves for Supercritical Flow : Symposium on High Velocity Flow'. *Transactions of American Society of Civil Engineers*, 1951.

6. F W Blaisdell. 'Graphical Construction of the Flow in a Transition by the Method of Characteristics'. *Soil Conservation Service Publication*, US Department of Agriculture, Minneapolis, 1946.

7. S U Vasudev. 'Numerical Investigations of Supercritical Flows'. Thesis submitted to Cornell University for Ph D degree, 1963.

8. J A Liggett and S U Vasudev. 'Slope and Friction Effects in Two-dimensional High-speed Channel Flow'. *Proceedings of 11th Congress of the International Association for Hydraulic Research*, Leningrad, vol 1, 1965.

9. A A Tursunov. 'The Methods of Governing of Geometrical Forms of Supercritical High Velocity Flows'. *Proceedings of 11th Congress of the international Association for Hydraulic Research*, Leningrad, vol 1, 1965.

10. J B Herbich and P Walsh. 'Supercritical Flow in Rectangular Expansions'. *Proceedings of American Society of Civil Engineers, Journal of the Hydraulic Division*, September 1972.